

Exchange Broadening Underlies the Enhancement of IDE-Dependent Degradation of Insulin by Anionic Membranes

Qiuchen Zheng,[†] Bethany Lee,[†] Micheal T. Kebede,[†] Valerie A. Ivancic, Merc M. Kemeh, Henrique Lemos Brito, Donald E. Spratt, and Noel D. Lazo*



Cite This: *ACS Omega* 2022, 7, 24757–24765



Read Online

ACCESS |



Metrics & More

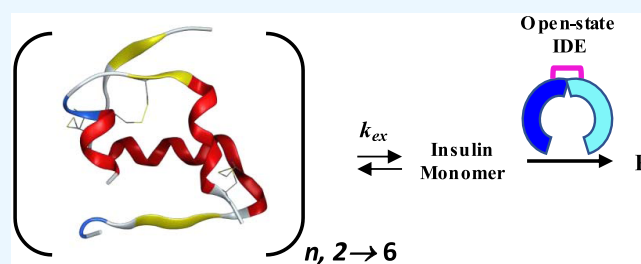


Article Recommendations



Supporting Information

ABSTRACT: Insulin-degrading enzyme (IDE) is an evolutionarily conserved ubiquitous zinc metalloprotease implicated in the efficient degradation of insulin monomer. However, IDE also degrades monomers of amyloidogenic peptides associated with disease, complicating the development of IDE inhibitors. In this work, we investigated the effects of the lipid composition of membranes on the IDE-dependent degradation of insulin. Kinetic analysis based on chromatography and insulin's helical circular dichroic signal showed that the presence of anionic lipids in membranes enhances IDE's activity toward insulin. Using NMR spectroscopy, we discovered that exchange broadening underlies the enhancement of IDE's activity. These findings, together with the adverse effects of anionic membranes in the self-assembly of IDE's amyloidogenic substrates, suggest that the lipid composition of membranes is a key determinant of IDE's ability to balance the levels of its physiologically and pathologically relevant substrates and achieve proteostasis.



INTRODUCTION

Insulin-degrading enzyme (IDE) is a ubiquitous zinc metalloprotease that has been implicated in the regulation of the steady-state levels of physiologically and pathologically important proteins, making it an appealing target for the development of therapeutic strategies for two common late-onset diseases: type 2 diabetes (T2D) and Alzheimer's disease (AD).^{1–3} IDE's substrates include key metabolic hormones (e.g., insulin and glucagon) and amyloidogenic peptides (e.g., islet amyloid polypeptide (IAPP) linked to T2D⁴ and A β 42 associated with AD⁵). Of this diverse array of substrates, kinetic studies have shown that IDE is highly effective at degrading insulin.^{6,7}

Since its discovery in 1949,⁸ several key structural features of IDE have been identified. IDE is composed of an N-terminal domain (IDE-N) and a C-terminal domain (IDE-C) (Figure 1) that come together to form a catalytic chamber, the volume of which limits the substrate to a monomer less than 80 residues in size.^{9,10} The enzyme exists in two major conformational states during its catalytic cycle:^{1,11} open-state IDE facilitates substrate capture and product release, and closed-state IDE allows proteolysis to take place. In addition to size, specificity is also provided by specific interactions between the substrate and IDE's exosite located \sim 30 Å away from the catalytic Zn²⁺ ion.^{7,10,12} Allosteric regulation of IDE's activity has been shown to be driven by endogenous molecules, including ATP,^{13,14} carnosine,¹⁵ dynorphin,¹⁶ somatostatin,¹⁷ and bradykinin.¹⁶ Kurochkin et al. showed that allosteric

mutagenesis can be an attractive strategy for increasing the activity of IDE toward A β .¹⁸ More recently, we showed that resveratrol sustains IDE's activity toward A β 42¹⁹ but has no effect on the enzyme's ability to degrade insulin,²⁰ suggesting that resveratrol is a substrate-selective activator of IDE. In spite of the structural and mechanistic advances discussed above, however, outstanding challenges remain in current efforts to develop IDE-centric therapeutics for T2D and AD. Importantly, regulatory processes that govern IDE's ability to degrade its monomeric substrates in physiological and pathological settings are not understood.

The subcellular localization of IDE *in vivo* is not well known.²¹ Nonetheless, *in vitro* studies have shown that the enzyme is localized primarily in the cytosol, as discussed in recent reviews.^{1,3} IDE has also been found to be associated with assemblies that contain lipid bilayers, including the cell membrane^{22–26} and membrane-enclosed organelles, including peroxisomes^{27–29} and endosomes.³⁰ IDE may also be present in the extracellular space in association with exosomes^{31–34} that also contain lipid bilayers.³⁵ The presence of IDE in the extracellular space seems to be well supported by several *in*

Received: May 3, 2022

Accepted: June 13, 2022

Published: July 7, 2022



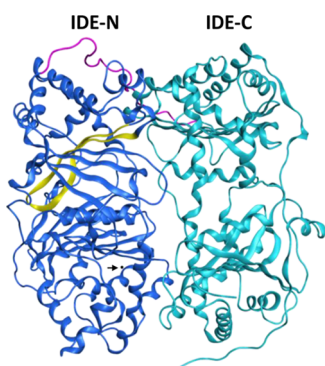


Figure 1. Closed conformational state of the insulin-degrading enzyme (PDB ID: 2WBY). IDE is composed of an N-terminal half (IDE-N) and a C-terminal half (IDE-C) joined together by an unstructured linker (magenta). When in its closed conformation, IDE forms a catalytic chamber that can only accommodate small monomeric substrates such as insulin and A β 42. IDE-N contains a conserved exosite (yellow), which has been hypothesized to anchor the substrate prior to degradation. IDE has the HXXEH motif, which contains the two histidine residues (H108 and H112) that coordinate Zn $^{2+}$ and the catalytically important glutamate residue (E111). The arrow in the lower half of IDE-N indicates the relative location of the catalytic Zn $^{2+}$ ion.

in vitro proteolysis studies. Selkoe and co-workers^{36–38} and Hersh and colleagues³⁹ identified IDE as the primary protease responsible for the degradation of A β secreted from neuronal and non-neuronal cells.

Insulin is a hormone that is essential for the metabolism of glucose.⁴⁰ It is a predominantly α -helical protein that is stored as a hexamer in β -cell secretory granules, presumably to protect it from unregulated or unwanted degradation.⁴¹ The key steps in the physiological journey of insulin in the body are:^{42,43} (a) secretion from β cells; (b) clearance in the liver where 75–80% of secreted insulin is cleared; (c) distribution to target tissues where it promotes glucose uptake; and (d) degradation in the kidney. The functional form of the protein is a monomer that initiates its function by binding to its membrane receptor.^{44–46} Interestingly, the binding of insulin to its receptor is also the initial step in its clearance by the liver.^{47–49} Two clearance pathways have been proposed. In the extracellular pathway, insulin is degraded by IDE without internalization of the substrate.^{26,50,51} In the intracellular pathway, some of the receptor-bound insulin is shunted to the endolysosomal system for degradation,^{52,53} where IDE degrades insulin in the neutral environment of early endosomes.^{30,54}

Regulatory mechanisms that underlie the dissociation of insulin monomer from hexameric insulin—important for its function and degradation—are not well understood. Here, we show that membranes that contain anionic lipids significantly enhance the IDE-dependent degradation of insulin through a mechanism that involves increased chemical exchange between insulin oligomers and degradable insulin monomer.

RESULTS AND DISCUSSION

Recombinant human IDE was expressed and purified in-house, as previously described.^{7,19,55} Small unilamellar vesicles (SUVs) of varying lipid compositions, including 100% zwitterionic DOPC (1,2-dioleoyl-*sn*-glycero-3-phosphocholine), 100% anionic DOPS (1,2-dioleoyl-*sn*-glycero-3-phospho-L-serine), and DOPC/DOPS (7:3 mol/mol), which mimics the ratio of zwitterionic to anionic lipids found in

cells relevant to metabolism including insulin-producing β cells,⁵⁶ were also prepared. We use SUVs as model membranes in our *in vitro* studies of the biophysical and biochemical properties of amyloidogenic proteins such as insulin and A β because of their high membrane curvatures that facilitate biologically relevant membrane-induced protein conformational transitions.⁵⁷ Insulin solutions were prepared at pH 7.4. At this pH and in the presence of Zn $^{2+}$, it is well known that insulin self-assembles to hexamers.^{58,59} In our hands, we found that the dominant oligomeric state of insulin depends on its concentration. Analytical gel filtration indicates that as the concentration of insulin was increased from 15 to 170 μ M, the dominant oligomeric state of insulin changes from dimers to hexamers (Figure S1).

The IDE-dependent degradation of insulin was carried out at 37 $^{\circ}$ C. Figure S2 presents time-dependent circular dichroic spectra showing that IDE remains active at 37 $^{\circ}$ C for 48 h. To quantitatively assess the effect of SUVs on the IDE-dependent degradation of insulin, we used a combination of chromatographic and spectroscopic techniques. Figure S3 presents representative time-dependent chromatograms of quenched insulin digestion reactions in the absence or presence of SUVs. Each data set shows the gradual loss of the insulin peak accompanied by the appearance of peaks at short retention times, consistent with proteolysis of the substrate. The amount of undigested insulin was determined using eq 1

$$\begin{aligned} \text{undigested insulin (\%)} \\ = \frac{\text{area of insulin peak at specific time point}}{\text{area of the insulin peak in the absence of IDE}} \times 100\% \end{aligned} \quad (1)$$

and plotted against digestion time, as shown in Figure S4. We noted that the loss of insulin with digestion time in samples that contain SUVs composed of 100% DOPC is similar to that in control samples which do not contain SUVs. In contrast, insulin in the presence of SUVs containing anionic DOPS was degraded more rapidly in a manner that correlates with the anionic lipid content of the vesicles. Figure S4 shows that after 1 h of digestion, <10 and \sim 45% of insulin remains in digests that contain SUVs composed of 100% DOPS and DOPC/DOPS (7:3 mol/mol), respectively. In contrast, almost 60% of insulin remain in samples that contain SUVs composed of 100% DOPC and in samples that do not contain SUVs.

Next, we determined the Michaelis–Menten kinetic constants for the IDE-dependent degradation of insulin using circular dichroism (CD) spectroscopy. Recently, we demonstrated that the dichroic spectrum of insulin is sensitive to the kinetics of its proteolysis by IDE.^{7,60} As degradation proceeded, the intensity of insulin's ellipticity at 222 nm, widely used as a measure of the helical content of proteins,^{61,62} decreased with an increase in digestion time.⁷ We calculated the amount of digested insulin using eq 2

$$[\text{DI}]_t = [\text{I}]_0 \times \left(1 - \frac{[\theta_{\text{obs}(222 \text{ nm})}]_t}{[\theta_{\text{obs}(222 \text{ nm})}]_0} \right) \quad (2)$$

where $[\text{DI}]_t$ is the amount of digested insulin at time t , $[\text{I}]_0$ is the initial amount of undigested insulin, and $[\theta_{\text{obs}(222 \text{ nm})}]_t$ and $[\theta_{\text{obs}(222 \text{ nm})}]_0$ are the observed ellipticities at time t and time = 0, respectively. Linear regression analysis of the plot of $[\text{DI}]_t$ against digestion time yielded V_0 , the initial rate of insulin proteolysis.⁷ Figure 2 shows that V_0 plotted against insulin

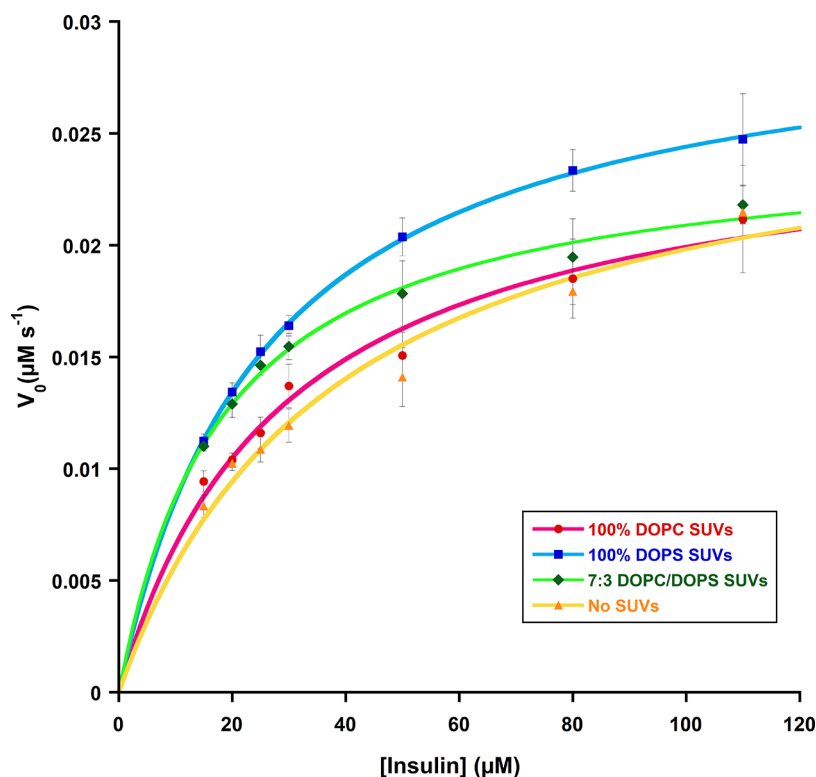


Figure 2. IDE-dependent degradation of insulin in the absence or presence of SUVs follows Michaelis–Menten kinetics. Plots of V_0 against insulin concentration are hyperbolic. Each data point represents the mean from three kinetic trials, and the error bars are standard deviations. The lines are fits to the Michaelis–Menten equation.

Table 1. Steady-State Kinetic Parameters for the IDE-Dependent Degradation of Insulin in the Absence and Presence of SUVs

SUVs	K_M (M)	k_{cat} (s^{-1})	k_{cat}/K_M ($M^{-1} s^{-1}$)
none	$3.8 \pm 0.3 \times 10^{-5}$	0.027 ± 0.0006	$7.2 \pm 0.5 \times 10^2$
100% DOPC	$3.2 \pm 0.5 \times 10^{-5}$	0.027 ± 0.003	$8.5 \pm 0.5 \times 10^2$
100% DOPS	$2.1 \pm 0.4 \times 10^{-5}$	0.028 ± 0.001	$1.4 \pm 0.03 \times 10^3$
DOPC/DOPS (7:3 mol/mol)	$2.1 \pm 0.03 \times 10^{-5}$	0.026 ± 0.0009	$1.2 \pm 0.05 \times 10^3$

concentration resulted in a hyperbolic plot fitted by the Michaelis–Menten equation. Table 1 presents the steady-state kinetic constants K_M (Michaelis constant), k_{cat} (turnover number), and k_{cat}/K_M obtained from the Michaelis–Menten plots. IDE's catalytic efficiency, indicated by k_{cat}/K_M , in the presence of SUVs composed of 100% DOPC was similar to the control. However, IDE's efficiency increased by 67 and 94% in the presence of SUVs composed of DOPC/DOPS (7:3 mol/mol) and 100% DOPS, respectively. Together, our kinetic analysis based on chromatography (Figure S3) and insulin's helical circular dichroic signal (Figure 2) show that membranes containing anionic lipids enhance the IDE-dependent degradation of insulin.

To explain the increased rate of insulin degradation in the presence of anionic lipids, we used solution-state 1H NMR spectroscopy. Insulin solutions at a concentration of 100 μM were prepared in deuterated buffer to prevent H_2O -peak-induced distortion of the peaks from insulin. We noted that the aromatic region (i.e., 6.6–7.4 ppm) of the 1H NMR spectra of the insulin digests is most sensitive to degradation. First, we determined the sensitivity of 1H NMR to the kinetics of degradation by IDE. Figure 3 presents portions of the 1H NMR spectra of insulin digests in the absence and presence of SUVs. In the absence of IDE, the peaks in the aromatic regions

of the spectra are broad. In the presence of IDE, the broad peaks are increasingly replaced by sharp peaks with digestion time, consistent with the production of insulin fragments that tumble rapidly in solution. The spectra of the digests in the absence of SUVs (Figure 3A) are similar to the spectra recorded for the samples that contain 100% DOPC SUVs (Figure 3B). Furthermore, the intensities of the sharp peaks in the 3-h spectra increase in the order of increasing amounts of DOPS, i.e., DOPC < DOPC/DOPS < DOPS, indicating that the degradation of insulin is enhanced by the presence of anionic lipids. Together, our NMR results are consistent with the kinetic results obtained by chromatographic (Figure S3) and circular dichroic spectroscopic methods (Figure 2 and Table 1).

Next, we analyzed the spectra of insulin in the absence of IDE to decipher the mechanism for the enhancement of degradation by anionic lipids. At a concentration of 100 μM , insulin in the presence of Zn^{2+} and at neutral pH exists mainly as a mixture of monomers and oligomers that are predominantly hexamers (Figure S1), consistent with results obtained by others using dynamic light scattering,⁶³ size-exclusion chromatography,⁶⁴ and analytical ultracentrifugation.⁶⁵ Because insulin at a concentration of 100 μM is degradable by IDE (Figure 3) and the enzyme only degrades

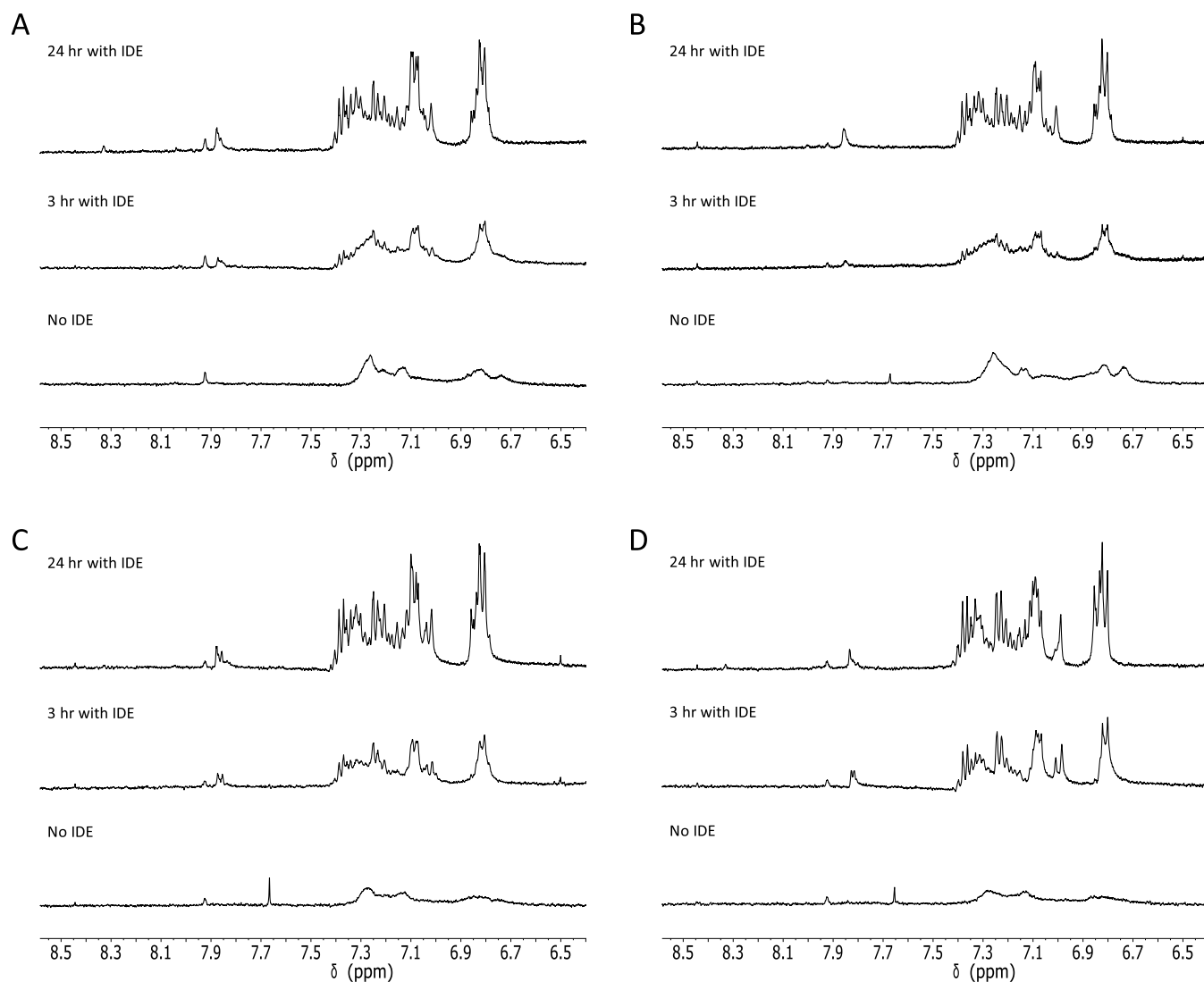


Figure 3. IDE-dependent degradation of insulin monitored by NMR. One-dimensional ^1H NMR spectra of insulin digestion reactions in (A) the absence of SUVs, and the presence of SUVs composed of (B) 100% DOPC, (C) DOPC/DOPS (7:3 mol/mol), and (D) 100% DOPS. In the absence of IDE, the broadening of the peaks in the aromatic region (6.6–7.4 ppm) in samples that contain membranes with anionic DOPS increased. In the presence of IDE, the broad peaks in the aromatic region are replaced by sharp peaks due to insulin fragments that tumble rapidly in solution. All spectra were recorded at 37 °C. The NMR samples were incubated at 37 °C in between the acquisition of spectra. The concentration of insulin in all samples was set at 100 μM . At this concentration, insulin exists mainly as hexamers. The insulin-to-lipid and the substrate-to-enzyme molar ratios were set at 1:50 and 100:1, respectively.

monomeric substrates,^{9,10} insulin monomer must be in dynamic exchange with insulin oligomers (Figure 4). Insulin monomer thus samples two environments: one in which it is in association with other molecules of itself and the other in which it is by itself. In NMR spectroscopy, this is known as chemical exchange,⁶⁶ also known as magnetic site exchange.⁶⁷ Chemical exchange is characterized by an exchange rate, denoted by k_{ex} (Figure 4). The relative values of k_{ex} and $\Delta\omega$, where $\Delta\omega$ is the difference in frequency between the two sites, define the slow and fast exchange limits of chemical exchange:

$$k_{\text{ex}} \ll \Delta\omega \quad \text{slow exchange}$$

$$k_{\text{ex}} \approx \Delta\omega \quad \text{intermediate exchange}$$

$$k_{\text{ex}} \gg \Delta\omega \quad \text{fast exchange}$$

Because the peaks in the aromatic region of the 1D ^1H NMR spectra of insulin in the absence of IDE are broad (Figure 3),

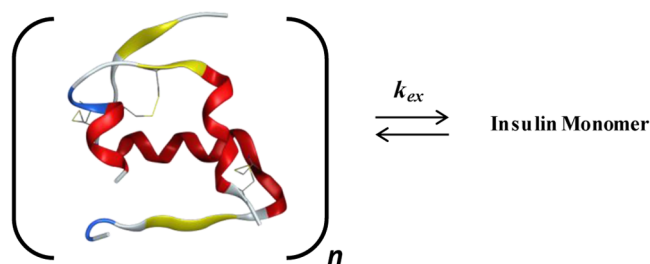


Figure 4. Chemical exchange in insulin. Oligomeric insulin and insulin monomer are in dynamic equilibrium with one another. This equilibrium is characterized by the exchange rate k_{ex} . The distribution of oligomers is indicated by n , which ranges from 2 to 6. At the concentration of insulin used in the NMR studies, hexamers are the dominant oligomers.

and sharp peaks expected for a protein of the size of the insulin monomer, i.e., ~5.8 kDa were not detected, the exchange between insulin oligomers and insulin monomers must be in the intermediate timescale. This conclusion is also supported by 2D NOESY NMR of insulin in the absence of IDE (Figure S5), which shows the absence of cross peaks due to insulin, in sharp contrast to NOESY spectra we reported for insulin at pH 2 in the absence of SUVs.⁶⁸ Additionally, our NOESY data (Figure S5) indicate that multidimensional relaxation-based NMR methods that were recently used to investigate the interaction of A β 42 with IDE do not apply.⁶⁹ In the presence of SUVs containing anionic lipids and in the absence of IDE, the broadening of the peaks in the aromatic regions of the spectra shown in Figure 3C,D increased. This is exchange broadening⁷⁰ that results from an increase in the exchange rate between insulin oligomers and insulin monomer. In turn, the increase in exchange rate leads to increased IDE-dependent degradation of insulin monomer.

Our work shows that the lipid composition of membranes is an efficient regulator of the dissociation of insulin monomer from oligomeric insulin and, thus, of the ensuing IDE-dependent degradation of insulin monomer. When anionic lipids are present, the exchange rate between insulin oligomer and insulin monomer increases, leading to increased availability of insulin monomer for degradation by IDE. Interestingly, levels of anionic phospholipids in islet cells increase significantly after glucose stimulation.⁷¹ We speculate that glucose stimulation *in vivo* also leads to an increase in anionic-phospholipid levels in β -cell membranes, resulting in increased release of insulin monomer.

Finally, in light of IDE's ability to degrade insulin, A β 42, and IAPP, it is no surprise that there has been a strong interest in the development of small molecules that modulate IDE's activity.^{1–3,72} Several inhibitors have been reported to elevate insulin levels in cells or mice, including BMD44768,⁷³ B35,⁷⁴ 6bk,⁷⁵ Ii1,⁷⁶ and P12-3A.⁷⁷ In spite of these significant advances, outstanding challenges remain.^{1–3,72} Most importantly, the inhibition of IDE may lead to increased levels of A β 42 and IAPP. Attractive strategies in response to this challenge include development of substrate-selective IDE inhibitors,⁷⁸ identification of allosteric ligands,⁷⁹ and allosteric mutagenesis of IDE.¹⁸ These strategies require consideration of the mechanisms that regulate the levels of the monomeric states of IDE's substrates. In the case of insulin, we have shown here that anionic lipids in membranes increase the levels of IDE-degradable insulin monomer. However, this finding does not apply to all of IDE's substrates. The self-assembly of IDE's amyloidogenic substrates has been shown to be enhanced by anionic lipids in membranes.^{4,57,80,81} Zhang et al. showed that even low levels of anionic lipids promote the aggregation of cationic IAPP and facilitate IAPP-induced leakage of membranes.⁸² Clusters of anionic GM1 gangliosides in membranes accelerate A β aggregation to form assemblies with increased cytotoxicity.⁸³ Aggregation is preceded by binding of A β to anionic lipids, which is mediated by cationic lysine residues (K16 and K28).^{84,85} The differential effects of anionic lipids in membranes in modulating the levels of the monomeric states of IDE's substrates indicate that the lipid composition of membranes is a key determinant of IDE's ability to balance the levels of its physiologically and pathologically relevant substrates. This finding should be considered in the development of IDE-centric therapeutic strategies for T2D and AD.

EXPERIMENTAL METHODS

Materials. Phospholipids, including 1,2-dioleoyl-*sn*-glycero-3-phosphocholine (DOPC) (>99% pure) and 1,2-dioleoyl-*sn*-glycero-3-phospho-L-serine (DOPS) (>99% pure) were purchased from Avanti Polar Lipids, Inc. (Alabaster, Alabama). Human insulin (99% pure, 0.4% zinc) was purchased from Sigma-Aldrich (St. Louis). Stock solutions of insulin were prepared in 10 mM phosphate buffer (pH 7.4). To overcome the low solubility of insulin at pH 7.4, the solutions were incubated overnight at 37 °C, followed by centrifugation for 1 min at 16 000g at room temperature to separate undissolved insulin. The concentration of insulin was determined by UV absorbance at 275 nm using a molar extinction coefficient of 6190 M⁻¹ cm⁻¹.⁶⁸

Analytical Gel Filtration Chromatography. Five insulin solutions with concentrations of 500, 300, 200, 100, 50, and 25 μ M in 50 mM Tris at pH 7.4 were prepared. To perform the chromatography, a precalibrated Superdex 75 HR 10/300 GL column connected to an ÄKTA pure FPLC system was used. The concentration of the fractions containing the sample that yielded maximum absorbance at 275 nm was determined by UV spectroscopy, as described above.

Preparation of Small Unilamellar Vesicles. SUVs containing 100% DOPC, 100% DOPS, or DOPC/DOPS (7:3 mol/mol) were prepared as previously described.⁵⁷ Briefly, lipids were dissolved in methanol/chloroform (1:1, v/v). After drying, the lipid films were hydrated with 1 mL of 10 mM phosphate buffer (pH 7.4). The resulting suspension of multilamellar vesicles was then subjected to 10 freeze–thaw cycles to increase their size homogeneity. This was followed by sonication using a VCX750 Vibra-Cell ultrasonic liquid processor equipped with a tapered microtip (Sonics and Materials, Inc., Newtown, CT) to produce SUVs. The SUVs were separated from titanium particles by centrifugation for 15 min at 16 000g at room temperature.

IDE Overexpression and Purification. Recombinant human IDE was expressed and purified as previously described.^{7,19,55} Briefly, glutathione-S-transferase tagged IDE (GST-IDE) was overexpressed in *E. coli* BL21-CodonPlus RIL cells. After cell lysis, GST-IDE was separated using a GStrap Fast Flow column connected to an ÄKTA pure FPLC system and eluted with phosphate-buffered saline containing 10 mM glutathione. GST PreScission protease was then used to cleave the GST tag. IDE was further purified using standard gel filtration.^{7,19,55} The concentration of IDE was determined by UV absorbance at 280 nm using its molar extinction coefficient of 113 570 M⁻¹ cm⁻¹.⁸⁶

IDE-Dependent Degradation of Insulin Monitored by Reversed-Phase HPLC. Four proteolysis samples, each with a total volume of 300 μ L, were prepared in triplicates. These samples included (1) insulin in the absence of SUVs; (2) insulin in the presence of 100% DOPC SUVs; (3) insulin in the presence of 100% DOPS SUVs; and (4) insulin in the presence of DOPC/DOPS (7:3 mol/mol) SUVs. The concentration of insulin was set at 40 μ M. The ratio of insulin to lipid was set at 1:50 (mol/mol). The substrate-to-enzyme ratio was set at 100:1 (mol/mol). IDE was added last to initiate the reaction, followed by incubation of the reaction solutions at 37 °C. At the 1-min, 1-h, 3-h, 6-h, 24-h, and 48-h time points of proteolysis, 50 μ L of the reaction solution was removed and transferred into an Eppendorf tube containing 23

μL of 1% (v/v) trifluoroacetic acid in water to quench the reaction.

All quenched samples were analyzed using a Varian ProStar 210 HPLC system equipped with a ProStar 325 Variable Wavelength UV–Visible Detector. Fractionation of insulin digests was carried out at room temperature using an Agilent AdvanceBio mAb C4 column. Solvent A was 0.1% (v/v) formic acid in H_2O , whereas solvent B was 0.1% (v/v) formic acid in acetonitrile. Water used for the mobile phase was obtained by a Millipore Milli-Q 185 Plus system (Millipore, Bedford, MA). Acetonitrile of chromatographic grade was supplied by Fisher Scientific. Aliquots (20 μL) of solutions of quenched insulin digests were injected into the HPLC manually and eluted with a 15-min linear gradient of 0–100% B at a flow rate of 1 mL/min. Elution of analytes was monitored by UV absorbance at wavelengths 214 and 254 nm. By utilizing the integrals of the insulin peak, the amount of undigested insulin remaining at a specific time point of the proteolysis reaction was calculated using eq 1 and plotted against digestion time.

Kinetics of IDE-Dependent Degradation of Insulin by Circular Dichroism Spectroscopy. To obtain the steady-state kinetic parameters for the IDE-dependent degradation of insulin in the presence of SUVs, we used a kinetic assay that takes advantage of the loss of insulin's helical circular dichroic signal at 222 nm with digestion time.⁷ Briefly, seven insulin solutions in 10 mM phosphate buffer (pH 7.4) with concentrations ranging from 15 to 110 μM (i.e., 15, 20, 25, 30, 50, 80, and 110 μM) were prepared. The insulin solutions were prepared in the absence and presence of SUVs with the insulin/lipid ratio set at 1:50 (mol/mol). The reaction was initiated with the addition of IDE at a concentration of 1 μM . After mixing, the solution was transferred into a quartz cuvette with a path length of 1 mm and loaded into the sample holder of our JASCO J-815 spectropolarimeter set at 37 °C. The ellipticity at 222 nm ($[\theta_{\text{obs}}(222\text{ nm})]$) was then recorded for 5 min. The real-time $[\theta_{\text{obs}}(222\text{ nm})]$ data were then used to calculate the amount of digested insulin ([DI]) using eq 2. Linear regression analysis of plots of $[\text{DI}]_t$ against digestion time (up to 5 min) yielded V_0 , the initial rate or velocity of the IDE-catalyzed degradation of insulin. Michaelis–Menten plots were then generated, from which the kinetic constants K_M , V_{max} , k_{cat} , and k_{cat}/K_M were determined by curve-fitting to the Michaelis–Menten equation (eq 3)

$$V_0 = \frac{V_{\text{max}}[\text{S}]}{K_M + [\text{S}]} \quad (3)$$

IDE-Dependent Degradation of Insulin Monitored by ^1H NMR Spectroscopy. Stock solutions of insulin and SUVs in 10 mM phosphate buffer were prepared using 99.9% D_2O (Sigma-Aldrich). The concentration of insulin in all NMR samples was set at 100 μM . In samples that contain SUVs, the insulin/lipid ratio was set at 1:50 (mol/mol). The substrate/enzyme ratio was set at 100:1 (mol/mol). All 1D and 2D ^1H NMR spectra were recorded at 37 °C using a Varian INOVA spectrometer operating at 400 MHz. For chemical shift referencing, the methyl peak of the internal standard 2,2-dimethyl-2-silapentane-5-sulfonate was set to 0 ppm. NOESY spectra were recorded in phase-sensitive mode using mixing times ranging from 100 to 400 ms. All samples were incubated at 37 °C in between spectral acquisitions.

■ ASSOCIATED CONTENT

Supporting Information

The Supporting Information is available free of charge at <https://pubs.acs.org/doi/10.1021/acsomega.2c02747>.

Analytical gel filtration of insulin at pH 7.4 (Figure S1); far UV circular dichroic spectra of insulin as a function of digestion time at 37 °C (Figure S2); IDE-dependent degradation of insulin monitored by reversed-phase HPLC (Figure S3); dependence of the amount of undigested insulin on digestion time (Figure S4); and 2D NOESY spectra of insulin in the presence of SUVs composed of 100% DOPS (Figure S5) (PDF)

■ AUTHOR INFORMATION

Corresponding Author

Noel D. Lazo – *Gustaf H. Carlson School of Chemistry and Biochemistry, Clark University, Worcester, Massachusetts 01610, United States*; orcid.org/0000-0003-1769-7572; Email: nlazo@clarku.edu

Authors

Qiuchen Zheng – *Gustaf H. Carlson School of Chemistry and Biochemistry, Clark University, Worcester, Massachusetts 01610, United States*

Bethany Lee – *Gustaf H. Carlson School of Chemistry and Biochemistry, Clark University, Worcester, Massachusetts 01610, United States*

Micheal T. Kebede – *Gustaf H. Carlson School of Chemistry and Biochemistry, Clark University, Worcester, Massachusetts 01610, United States*

Valerie A. Ivancic – *Gustaf H. Carlson School of Chemistry and Biochemistry, Clark University, Worcester, Massachusetts 01610, United States*

Merc M. Kemeh – *Gustaf H. Carlson School of Chemistry and Biochemistry, Clark University, Worcester, Massachusetts 01610, United States*

Henrique Lemos Brito – *Gustaf H. Carlson School of Chemistry and Biochemistry, Clark University, Worcester, Massachusetts 01610, United States*

Donald E. Spratt – *Gustaf H. Carlson School of Chemistry and Biochemistry, Clark University, Worcester, Massachusetts 01610, United States*

Complete contact information is available at: <https://pubs.acs.org/10.1021/acsomega.2c02747>

Author Contributions

[†]Q.Z., B.L., and M.T.K. contributed equally to this work. All authors have given approval to the final version of the manuscript.

Funding

This work was supported by the National Institute on Aging Grant R15AG055043 to N.D.L.

Notes

The authors declare no competing financial interest.

■ ACKNOWLEDGMENTS

The authors thank Prof. Malcolm A. Leissring (the University of California at Irvine) for the bacterial expression vector encoding IDE fused to GST.

REFERENCES

- (1) Tang, W. J. Targeting insulin-degrading enzyme to treat type 2 diabetes mellitus. *Trends Endocrinol. Metab.* **2016**, *27*, 24–34.
- (2) Kurochkin, I. V.; Guarnera, E.; Berezovsky, I. N. Insulin-degrading enzyme in the fight against Alzheimer's disease. *Trends Pharmacol. Sci.* **2018**, *39*, 49–58.
- (3) Leissring, M. A.; Gonzalez-Casimiro, C. M.; Merino, B.; Suire, C. N.; Perdomo, G. Targeting insulin-degrading enzyme in insulin clearance. *Int. J. Mol. Sci.* **2021**, *22*, 2235.
- (4) Milardi, D.; Gazit, E.; Radford, S. E.; Xu, Y.; Gallardo, R. U.; Caflich, A.; Westermarck, G. T.; Westermarck, P.; Rosa, C.; Ramamoorthy, A. Proteostasis of islet amyloid polypeptide: A molecular perspective of risk factors and protective strategies for type II diabetes. *Chem. Rev.* **2021**, *121*, 1845–1893.
- (5) Selkoe, D. J.; Hardy, J. The amyloid hypothesis of Alzheimer's disease at 25 years. *EMBO Mol. Med.* **2016**, *8*, 595–608.
- (6) Chesneau, V.; Rosner, M. R. Functional human insulin-degrading enzyme can be expressed in bacteria. *Protein Expression Purif.* **2000**, *19*, 91–98.
- (7) Ivancic, V. A.; Krasinski, C. A.; Zheng, Q.; Meservier, R. J.; Spratt, D. E.; Lazo, N. D. Enzyme kinetics from circular dichroism of insulin reveals mechanistic insights into the regulation of insulin-degrading enzyme. *Biosci. Rep.* **2018**, *38*, No. BSR20181416.
- (8) Mirsky, I. A.; Broh-Kahn, R. H. The inactivation of insulin by tissue extracts; the distribution and properties of insulin inactivating extracts. *Arch. Biochem.* **1949**, *20*, 1–9.
- (9) Shen, Y.; Joachimiak, A.; Rosner, M. R.; Tang, W. J. Structures of human insulin-degrading enzyme reveal a new substrate recognition mechanism. *Nature* **2006**, *443*, 870–874.
- (10) Manolopoulou, M.; Guo, Q.; Malito, E.; Schilling, A. B.; Tang, W. J. Molecular basis of catalytic chamber-assisted unfolding and cleavage of human insulin by human insulin-degrading enzyme. *J. Biol. Chem.* **2009**, *284*, 14177–14188.
- (11) Zhang, Z.; Liang, W. G.; Bailey, L. J.; Tan, Y. Z.; Wei, H.; Wang, A.; Farcasanu, M.; Woods, V. A.; McCord, L. A.; Lee, D.; Shang, W.; et al. Ensemble cryoEM elucidates the mechanism of insulin capture and degradation by human insulin degrading enzyme. *eLife* **2018**, *7*, No. e33572.
- (12) Malito, E.; Ralat, L. A.; Manolopoulou, M.; Tsay, J. L.; Wadlington, N. L.; Tang, W. J. Molecular bases for the recognition of short peptide substrates and cysteine-directed modifications of human insulin-degrading enzyme. *Biochemistry* **2008**, *47*, 12822–12834.
- (13) Im, H.; Manolopoulou, M.; Malito, E.; Shen, Y.; Zhao, J.; Neant-Fery, M.; Sun, C. Y.; Meredith, S. C.; Sisodia, S. S.; Leissring, M. A.; Tang, W. J. Structure of substrate-free human insulin-degrading enzyme (IDE) and biophysical analysis of ATP-induced conformational switch of IDE. *J. Biol. Chem.* **2007**, *282*, 25453–25463.
- (14) Song, E. S.; Juliano, M. A.; Juliano, L.; Fried, M. G.; Wagner, S. L.; Hersh, L. B. ATP effects on insulin-degrading enzyme are mediated primarily through its triphosphate moiety. *J. Biol. Chem.* **2004**, *279*, 54216–54220.
- (15) Distefano, A.; Caruso, G.; Oliveri, V.; Bellia, F.; Sbardella, D.; Zingale, G. A.; Caraci, F.; Grasso, G. Neuroprotective effect of carnosine is mediated by insulin-degrading enzyme. *ACS Chem. Neurosci.* **2022**, *13*, 1588–1593.
- (16) Song, E.-S.; Juliano, M. A.; Juliano, L.; Hersh, L. B. Substrate activation of insulin-degrading enzyme (insulysin). A potential target for drug development. *J. Biol. Chem.* **2003**, *278*, 49789–49794.
- (17) Ciaccio, C.; Tundo, G. R.; Grasso, G.; Spoto, G.; Marasco, D.; Ruvo, M.; Gioia, M.; Rizzarelli, E.; Coletta, M. Somatostatin: A novel substrate and a modulator of insulin-degrading enzyme activity. *J. Mol. Biol.* **2009**, *385*, 1556–15567.
- (18) Kurochkin, I. V.; Guarnera, E.; Wong, J. H.; Eisenhaber, F.; Berezovsky, I. N. Toward allosterically increased catalytic activity of insulin-degrading enzyme against amyloid peptides. *Biochemistry* **2017**, *56*, 228–239.
- (19) Krasinski, C. A.; Ivancic, V. A.; Zheng, Q.; Spratt, D. E.; Lazo, N. D. Resveratrol sustains insulin-degrading enzyme activity toward A β 42. *ACS Omega* **2018**, *3*, 13275–13282.
- (20) Zheng, Q.; Kebede, M. T.; Lee, B.; Krasinski, C. A.; Islam, S.; Wurfl, L. A.; Kemeh, M. M.; Ivancic, V. A.; Jakobsche, C. E.; Spratt, D. E.; Lazo, N. D. Differential effects of polyphenols on insulin proteolysis by the insulin-degrading enzyme. *Antioxidants* **2021**, *10*, 1342.
- (21) Leissring, M. A. Insulin-degrading enzyme: Paradoxes and possibilities. *Cells* **2021**, *10*, 2445.
- (22) Li, Q.; Ali, M. A.; Cohen, J. I. Insulin degrading enzyme is a cellular receptor mediating varicella-zoster virus infection and cell-to-cell spread. *Cell* **2006**, *127*, 305–316.
- (23) Bulloj, A.; Leal, M. C.; Surace, E. I.; Zhang, X.; Xu, H.; Ledesma, M. D.; Castano, E. M.; Morelli, L. Detergent resistant membrane-associated IDE in brain tissue and cultured cells: Relevance to A β and insulin degradation. *Mol. Neurodegener.* **2008**, *3*, 22.
- (24) Duckworth, W. C.; Bennett, R. G.; Hamel, F. G. Insulin degradation: Progress and potential. *Endocr. Rev.* **1998**, *19*, 608–624.
- (25) Yokono, K.; Imamura, Y.; Sakai, H.; Baba, S. Insulin-degrading activity of plasma membranes from rat skeletal muscle: Its isolation, characterization, and biologic significance. *Diabetes* **1979**, *28*, 810–817.
- (26) Goldfine, I. D.; Williams, J. A.; Bailey, A. C.; Wong, K. Y.; Iwamoto, Y.; Yokono, K.; Baba, S.; Roth, R. A. Degradation of insulin by isolated mouse pancreatic acini. Evidence for cell surface protease activity. *Diabetes* **1984**, *33*, 64–72.
- (27) Kuo, W. L.; Gehm, B. D.; Rosner, M. R.; Li, W.; Keller, G. Inducible expression and cellular localization of insulin-degrading enzyme in a stably transfected cell line. *J. Biol. Chem.* **1994**, *269*, 22599–22606.
- (28) Authier, F.; Bergeron, J. J.; Ou, W. J.; Rachubinski, R. A.; Posner, B. I.; Walton, P. A. Degradation of the cleaved leader peptide of thiolase by a peroxisomal proteinase. *Proc. Natl. Acad. Sci. U.S.A.* **1995**, *92*, 3859–3863.
- (29) Morita, M.; Kurochkin, I. V.; Motojima, K.; Goto, S.; Takano, T.; Okamura, S.; Sato, R.; Yokota, S.; Imanaka, T. Insulin-degrading enzyme exists inside of rat liver peroxisomes and degrades oxidized proteins. *Cell Struct. Funct.* **2000**, *25*, 309–315.
- (30) Hamel, F. G.; Mahoney, M. J.; Duckworth, W. C. Degradation of intraendosomal insulin by insulin-degrading enzyme without acidification. *Diabetes* **1991**, *40*, 436–443.
- (31) Bulloj, A.; Leal, M. C.; Xu, H.; Castano, E. M.; Morelli, L. Insulin-degrading enzyme sorting in exosomes: A secretory pathway for a key brain amyloid- β degrading protease. *J. Alzheimer's Dis.* **2010**, *19*, 79–95.
- (32) Tamboli, I. Y.; Barth, E.; Christian, L.; Siepmann, M.; Kumar, S.; Singh, S.; Tolksdorf, K.; Heneka, M. T.; Lutjohann, D.; Wunderlich, P.; Walter, J. Statins promote the degradation of extracellular amyloid β -peptide by microglia via stimulation of exosome-associated insulin-degrading enzyme (IDE) secretion. *J. Biol. Chem.* **2010**, *285*, 37405–37414.
- (33) Mett, J.; Lauer, A. A.; Janitschke, D.; Griebisch, L. V.; Theiss, E. L.; Grimm, H. S.; Koivisto, H.; Tanila, H.; Hartmann, T.; Grimm, M. O. W. Medium-chain length fatty acids enhance A β degradation by affecting insulin-degrading enzyme. *Cells* **2021**, *10*, 2941.
- (34) Sanderson, R. D.; Bandari, S. K.; Vlodavsky, I. Proteases and glycosidases on the surface of exosomes: Newly discovered mechanisms for extracellular remodeling. *Matrix Biol.* **2019**, *75*–76, 160–169.
- (35) Skotland, T.; Hessvik, N. P.; Sandvig, K.; Llorente, A. Exosomal lipid composition and the role of ether lipids and phosphoinositides in exosome biology. *J. Lipid Res.* **2019**, *60*, 9–18.
- (36) Vekrellis, K.; Ye, Z.; Qiu, W. Q.; Walsh, D.; Hartley, D.; Chesneau, V.; Rosner, M. R.; Selkoe, D. J. Neurons regulate extracellular levels of amyloid β -protein via proteolysis by insulin-degrading enzyme. *J. Neurosci.* **2000**, *20*, 1657–1665.
- (37) Qiu, W. Q.; Ye, Z.; Kholodenko, D.; Seubert, P.; Selkoe, D. J. Degradation of amyloid β -protein by a metalloprotease secreted by microglia and other neural and non-neural cells. *J. Biol. Chem.* **1997**, *272*, 6641–6646.

- (38) Qiu, W. Q.; Walsh, D. M.; Ye, Z.; Vekrellis, K.; Zhang, J.; Podlisny, M. B.; Rosner, M. R.; Safavi, A.; Hersh, L. B.; Selkoe, D. J. Insulin-degrading enzyme regulates extracellular levels of amyloid β -protein by degradation. *J. Biol. Chem.* **1998**, *273*, 32730–32738.
- (39) Mukherjee, A.; Song, E.; Ehmann, M. K.; Goodman, J. P.; St Pyrek, J.; Estus, S.; Hersh, L. B. Insulysin hydrolyzes amyloid β peptides to products that are neither neurotoxic nor deposit on amyloid plaques. *J. Neurosci.* **2000**, *20*, 8745–8749.
- (40) White, M. F.; Ronald Kahn, C. Insulin action at a molecular level - 100 years of progress. *Mol. Metab.* **2021**, *52*, No. 101304.
- (41) Blundell, T. L.; Cutfield, J. F.; Dodson, E. J.; Dodson, G. G.; Hodgkin, D. C.; Mercola, D. A. The crystal structure of rhombohedral 2 zinc insulin. *Cold Spring Harbor Symp. Quant. Biol.* **1972**, *36*, 233–241.
- (42) Tokarz, V. L.; MacDonald, P. E.; Klip, A. The cell biology of systemic insulin function. *J. Cell Biol.* **2018**, *217*, 2273–2289.
- (43) Najjar, S. M.; Perdomo, G. Hepatic insulin clearance: Mechanism and physiology. *Physiology* **2019**, *34*, 198–215.
- (44) Freychet, P.; Roth, J.; Neville, D. M., Jr. Insulin receptors in the liver: Specific binding of (125 I)insulin to the plasma membrane and its relation to insulin bioactivity. *Proc. Natl. Acad. Sci. U.S.A.* **1971**, *68*, 1833–1837.
- (45) Kasuga, M.; Zick, Y.; Blithe, D. L.; Crettaz, M.; Kahn, C. R. Insulin stimulates tyrosine phosphorylation of the insulin receptor in a cell-free system. *Nature* **1982**, *298*, 667–669.
- (46) Kasuga, M.; Karlsson, F. A.; Kahn, C. R. Insulin stimulates the phosphorylation of the 95,000-dalton subunit of its own receptor. *Science* **1982**, *215*, 185–187.
- (47) Terris, S.; Steiner, D. F. Binding and degradation of 125 I-insulin by rat hepatocytes. *J. Biol. Chem.* **1975**, *250*, 8389–8398.
- (48) Caro, J. F.; Muller, G.; Glennon, J. A. Insulin processing by the liver. *J. Biol. Chem.* **1982**, *257*, 8459–8466.
- (49) Michael, M. D.; Kulkarni, R. N.; Postic, C.; Previs, S. F.; Shulman, G. I.; Magnuson, M. A.; Kahn, C. R. Loss of insulin signaling in hepatocytes leads to severe insulin resistance and progressive hepatic dysfunction. *Mol. Cell* **2000**, *6*, 87–97.
- (50) Hamel, F. G.; Peavy, D. E.; Ryan, M. P.; Duckworth, W. C. HPLC analysis of insulin degradation products from isolated hepatocytes. Effects of inhibitors suggest intracellular and extracellular pathways. *Diabetes* **1987**, *36*, 702–708.
- (51) Yokono, K.; Roth, R. A.; Baba, S. Identification of insulin-degrading enzyme on the surface of cultured human lymphocytes, rat hepatoma cells, and primary cultures of rat hepatocytes. *Endocrinology* **1982**, *111*, 1102–1108.
- (52) Baldwin, D., Jr.; Prince, M.; Marshall, S.; Davies, P.; Olefsky, J. M. Regulation of insulin receptors: Evidence for involvement of an endocytotic internalization pathway. *Proc. Natl. Acad. Sci. U.S.A.* **1980**, *77*, 5975–5978.
- (53) Posner, B. I.; Khan, M. N.; Bergeron, J. J. Endocytosis of peptide hormones and other ligands. *Endocr. Rev.* **1982**, *3*, 280–298.
- (54) Yonezawa, K.; Yokono, K.; Shii, K.; Hari, J.; Yaso, S.; Amano, K.; Sakamoto, T.; Kawase, Y.; Akiyama, H.; Nagata, M.; Baba, S. Insulin-degrading enzyme is capable of degrading receptor-bound insulin. *Biochem. Biophys. Res. Commun.* **1988**, *150*, 605–614.
- (55) Krasinski, C. A.; Zheng, Q.; Ivancic, V. A.; Spratt, D. E.; Lazo, N. D. The longest amyloid- β precursor protein intracellular domain produced with A β 42 forms β -sheet-containing monomers that self-assemble and are proteolyzed by insulin-degrading enzyme. *ACS Chem. Neurosci.* **2018**, *9*, 2892–2897.
- (56) Engel, M. F. M.; Khemtouri, L.; Kleijer, C. C.; Meeldijk, H. J.; Jacobs, J.; Verkleij, A. J.; de Kruijff, B.; Killian, J. A.; Hoppener, J. W. Membrane damage by human islet amyloid polypeptide through fibril growth at the membrane. *Proc. Natl. Acad. Sci. U.S.A.* **2008**, *105*, 6033–6038.
- (57) Zheng, Q.; Carty, S. N.; Lazo, N. D. Helix dipole and membrane electrostatics delineate conformational transitions in the self-assembly of amyloidogenic peptides. *Langmuir* **2020**, *36*, 8389–8397.
- (58) Grant, P. T.; Coombs, T. L.; Frank, B. H. Differences in the nature of the interaction of insulin and proinsulin with zinc. *Biochem. J.* **1972**, *126*, 433–440.
- (59) Dunn, M. F. Zinc-ligand interactions modulate assembly and stability of the insulin hexamer – a review. *Biomaterials* **2005**, *18*, 295–303.
- (60) Grasso, G. Commentary on Ivancic *et al.*: Enzyme kinetics from circular dichroism of insulin reveals mechanistic insights into the regulation of insulin-degrading enzyme. *Biosci. Rep.* **2018**, *38*, No. BSR20181555.
- (61) Chen, Y. H.; Yang, J. T.; Chau, K. H. Determination of the helix and beta form of proteins in aqueous solution by circular dichroism. *Biochemistry* **1974**, *13*, 3350–3359.
- (62) Lazo, N. D.; Downing, D. T. Circular dichroism of model peptides emulating the amphipathic α -helical regions of intermediate filaments. *Biochemistry* **1997**, *36*, 2559–2565.
- (63) Attri, A. K.; Fernandez, C.; Minton, A. P. Self-association of Zn-insulin at neutral pH: Investigation by concentration gradient static and dynamic light scattering. *Biophys. Chem.* **2010**, *148*, 23–27.
- (64) Xu, Y.; Yan, Y.; Seeman, D.; Sun, L.; Dubin, P. L. Multimerization and aggregation of native-state insulin: Effect of zinc. *Langmuir* **2012**, *28*, 579–586.
- (65) Adams, G. G.; Meal, A.; Morgan, P. S.; Alzahrani, Q. E.; Zobel, H.; Lithgo, R.; Kok, M. S.; Besong, D. T. M.; Jiwani, S. I.; Ballance, S.; et al. Characterisation of insulin analogues therapeutically available to patients. *PLoS One* **2018**, *13*, No. e0195010.
- (66) Johnson, C. S. Chemical Rate Processes and Magnetic Resonance. In *Advances in Magnetic and Optical Resonance*; Academic Press, 1965; Vol. 1, pp 33–102.
- (67) Harris, R. K. *Nuclear Magnetic Resonance Spectroscopy: A Physicochemical View*; Longman Scientific and Technical: Essex, England, 1986; pp 119–141.
- (68) Zheng, Q.; Lazo, N. D. Mechanistic studies of the inhibition of insulin fibril formation by rosmarinic acid. *J. Phys. Chem. B* **2018**, *122*, 2323–2331.
- (69) Ramaraju, B.; Nelson, S. L.; Zheng, W.; Ghirlando, R.; Deshmukh, L. Quantitative NMR study of insulin-degrading enzyme using amyloid- β and HIV-1 p6 elucidates its chaperone activity. *Biochemistry* **2021**, *60*, 2519–2523.
- (70) Kaplan, J. L.; Fraenkel, G. *NMR of Chemically Exchanging Systems*; Academic Press: New York, 1980; pp 74–80.
- (71) Rustenbeck, I.; Matthies, A.; Lenzen, S. Lipid composition of glucose-stimulated pancreatic islets and insulin-secreting tumor cells. *Lipids* **1994**, *29*, 685–692.
- (72) González-Casimiro, C. M.; Merino, B.; Casanueva-Alvarez, E.; Postigo-Casado, T.; Camara-Torres, P.; Fernandez-Diaz, C. M.; Leissring, M. A.; Cozar-Castellano, I.; Perdomo, G. Modulation of insulin sensitivity by insulin-degrading enzyme. *Biomaterials* **2021**, *9*, 86.
- (73) Deprez-Poulain, R.; Hennuyer, N.; Bosc, D.; Liang, W. G.; Enee, E.; Marechal, X.; Charton, J.; Totobenazara, J.; Berte, G.; Jahklal, J.; et al. Catalytic site inhibition of insulin-degrading enzyme by a small molecule induces glucose intolerance in mice. *Nat. Commun.* **2015**, *6*, No. 8250.
- (74) Yang, D.; Qin, W.; Shi, X.; Zhu, B.; Xie, M.; Zhao, H.; Teng, B.; Wu, Y.; Zhao, R.; Yin, F.; Ren, P.; Liu, L.; Li, Z. Stabilized β -hairpin peptide inhibits insulin degrading enzyme. *J. Med. Chem.* **2018**, *61*, 8174–8185.
- (75) Maianti, J. P.; McFedries, A.; Foda, Z. H.; Kleiner, R. E.; Du, X. Q.; Leissring, M. A.; Tang, W. J.; Charron, M. J.; Seeliger, M. A.; Saghatelyan, A.; Liu, D. R. Anti-diabetic activity of insulin-degrading enzyme inhibitors mediated by multiple hormones. *Nature* **2014**, *511*, 94–98.
- (76) Abdul-Hay, S. O.; Lane, A. L.; Caulfield, T. R.; Claussin, C.; Bertrand, J.; Masson, A.; Choudhry, S.; Fauq, A. H.; Maharvi, G. M.; Leissring, M. A. Optimization of peptide hydroxamate inhibitors of insulin-degrading enzyme reveals marked substrate-selectivity. *J. Med. Chem.* **2013**, *56*, 2246–2255.

(77) Suire, C. N.; Nainar, S.; Fazio, M.; Kreutzer, A. G.; Paymozd-Yazdi, T.; Topper, C. L.; Thompson, C. R.; Leissring, M. A. Peptidic inhibitors of insulin-degrading enzyme with potential for dermatological applications discovered via phage display. *PLoS One* **2018**, *13*, No. e0193101.

(78) Maianti, J. P.; Tan, G. A.; Vetere, A.; Welsh, A. J.; Wagner, B. K.; Seeliger, M. A.; Liu, D. R. Substrate-selective inhibitors that reprogram the activity of insulin-degrading enzyme. *Nat. Chem. Biol.* **2019**, *15*, 565–574.

(79) Noinaj, N.; Bhasin, S. K.; Song, E. S.; Scoggin, K. E.; Juliano, M. A.; Juliano, L.; Hersh, L. B.; Rodgers, D. W. Identification of the allosteric regulatory site of insulysin. *PLoS One* **2011**, *6*, No. e20864.

(80) Matsuzaki, K. Physicochemical interactions of amyloid β -peptide with lipid bilayers. *Biochim. Biophys. Acta, Biomembr.* **2007**, *1768*, 1935–1942.

(81) Diociaiuti, M.; Bonanni, R.; Cariati, I.; Frank, C.; D’Arcangelo, G. Amyloid prefibrillar oligomers: The surprising commonalities in their structure and activity. *Int. J. Mol. Sci.* **2021**, *22*, 6435.

(82) Zhang, X.; St Clair, J. R.; London, E.; Raleigh, D. P. Islet amyloid polypeptide membrane interactions: Effects of membrane composition. *Biochemistry* **2017**, *56*, 376–390.

(83) Matsuzaki, K. $A\beta$ -ganglioside interactions in the pathogenesis of alzheimer’s disease. *Biochim. Biophys. Acta, Biomembr.* **2020**, *1862*, No. 183233.

(84) Tachi, Y.; Okamoto, Y.; Okumura, H. Conformational change of amyloid- β 40 in association with binding to GM1-glycan cluster. *Sci. Rep.* **2019**, *9*, No. 6853.

(85) Pilkington, A. W.; Schupp, J.; Nyman, M.; Valentine, S. J.; Smith, D. M.; Legleiter, J. Acetylation of $A\beta$ 40 alters aggregation in the presence and absence of lipid membranes. *ACS Chem. Neurosci.* **2020**, *11*, 146–161.

(86) Sharma, S. K.; Chorell, E.; Steneberg, P.; Vernersson-Lindahl, E.; Edlund, H.; Wittung-Stafshede, P. Insulin-degrading enzyme prevents α -synuclein fibril formation in a nonproteolytical manner. *Sci. Rep.* **2015**, *5*, No. 12531.